The Astronomical Journal, 136:899–908, 2008 September doi:10.1088/0004-6256/136/3/899

THE SOLAR NEIGHBORHOOD. XX. DISCOVERY AND CHARACTERIZATION OF 21 NEW NEARBY WHITE DWARF SYSTEMS

John P. Subasavage[1,5], Todd J. Henry[1,5], P. Bergeron[2], P. Dufour[3], and Nigel C. Hambly[4]
[1] Department of Physics and Astronomy, Georgia State University, Atlanta, GA 30302-4106, USA; subasavage@chara.gsu.edu, thenry@chara.gsu.edu
[2] Département de Physique, Université de Montréal, C.P. 6128, Succ. Centre-Ville, Montréal, Québec H3C 3J7, Canada; bergeron@astro.umontreal.ca
[3] Department of Astronomy and Steward Observatory, University of Arizona, 933 North Cherry Avenue, Tucson, AZ 85721, USA; dufourpa@as.arizona.edu
[4] Scottish Universities Physics Alliance (SUPA), Institute for Astronomy, University of Edinburgh, Royal Observatory, Blackford Hill, Edinburgh EH9 3HJ, Scotland, UK; nch@roe.ac.uk
Received 2008 April 16; accepted 2008 May 19; published 2008 July 21

ABSTRACT

We present medium-resolution spectroscopy and multi-epoch *VRI* photometry for 21 new nearby (<50 pc) white dwarf (WD) systems brighter than $V \sim 17$. Of the new systems, ten are DA (including a wide double-degenerate system with two DA components), eight are DC, two are DZ, and one is DB. In addition, we include multi-epoch *VRI* photometry for 11 known WD systems that do not have trigonometric parallax determinations. Using model atmospheres relevant for various types of WDs (depending on spectral signatures), we perform spectral energy distribution modeling by combining the optical photometry with the near-infrared (near-IR) JHK_S from the Two Micron All-Sky Survey to derive physical parameters (i.e., $T_{\rm eff}$ and distance estimates). We find that 12 new and six known WD systems are estimated to be within the NStars and Catalog of Nearby Stars (CNS) horizons of 25 pc. Coupled with identical analyses of the 56 WD systems presented in Paper XIX of this series, a total of 20 new WD systems and 18 known WD systems are estimated to be within 25 pc. These 38 systems of the 88 total studied represent a potential 34% increase in the 25 pc WD population (currently known to consist of 110 systems with trigonometric parallaxes of varying qualities). We continue an ongoing effort via Cerro Tololo Inter-American Observatory Parllax Investigation to measure trigonometric parallaxes for the systems estimated to be within 25 pc to confirm proximity and to further fill the incompleteness gap in the local WD population. Another 38 systems (both new and known) are estimated to be between 25 and 50 pc and are viable candidates for ground-based parallax efforts aiming to broaden the horizon of interest.

Key words: solar neighborhood – stars: distances – stars: evolution – stars: statistics – white dwarfs

1. INTRODUCTION

Given that all stars less than ~8 $M_\odot$ will eventually become white dwarfs (WDs), the study of this class of objects is vital to understanding our Galaxy. In particular, WD research addresses questions concerning stellar structure and evolution, Galactic components (i.e., thin disk, thick disk, halo), and even dark matter. The oldest (i.e., coolest and least luminous) WDs help to constrain the age of the Galactic components (particularly the thick disk) but shine feebly and are only visible and easily characterized if they are in our solar neighborhood. A complete volume-limited sample provides accurate statistics that can be reliably applied to the rest of the Galaxy to infer the WD mass fraction, contribution to the halo population, and WD number density within the disk. Interesting candidates can be targeted and more thoroughly scrutinized to identify unusual and astrophysically compelling systems.

In a continuing effort to further complete the nearby WD sample, we present spectra, optical, and near-IR photometry, as well as modeled physical parameters for 21 new WD systems in the southern hemisphere brighter than $V \sim 17$. Of these, 12 are estimated to be within 25 pc, the horizon of the Catalog of Nearby Stars (CNS; Gliese & Jahreiß 1991) and the NStars Database (Henry et al. 2003). In addition, six previously known WDs without trigonometric parallaxes are estimated to be within 25 pc.

[5] Visiting astronomer, Cerro Tololo Inter-American Observatory, National Optical Astronomy Observatory, which is operated by the Association of Universities for Research in Astronomy, under contract with the National Science Foundation.

2. CANDIDATE SELECTION

We conducted a southern hemisphere proper motion search using digitized scans of the SuperCOSMOS Sky Survey (SSS), adopting a faint magnitude limit of $R_{59F} = 16.5$, called the SuperCOSMOS-RECONS (SCR) survey. The first wave of the survey adopted a lower proper motion limit of 0.″40 yr^{-1} with new discoveries published in Hambly et al. (2004), Henry et al. (2004), and Subasavage et al. (2005a, 2005b). A second effort conducted by Finch et al. (2007) surveyed objects with proper motions from 0.18 to 0.″40 yr^{-1} and covered decl. −47° to −90°. The WD candidate selection effort also adopted the lower proper motion limit of 0.″18 yr^{-1}, yet reached farther north to decl. = 00°. Thus, this effort covered 92% of the southern sky, avoiding a few regions near the Galactic plane and the Magellanic Clouds (see Figure 1 of Subasavage et al. 2005b). A full discussion of the search methodology can be found in Hambly et al. (2004). Briefly, each of the four plate scans used (B_J, $R_{\rm ESO}$, R_{59F}, $I_{\rm IVN}$) were positionally mapped to a common coordinate system. Any object that appeared on all four plates and had a proper motion less than the lower limit was discarded. Objects that remained were then searched out to a radius defined by a proper motion of 10.″00 yr^{-1} and over 360° for any other unpaired objects. After a series of automated sifts for false pairings, the remaining objects were cross-referenced with previous proper motion catalogs to identify new and known objects.

Near-IR JHK_S magnitudes were extracted from the Two Micron All-Sky Survey (2MASS) for all real objects (new and known) and a reduced proper motion (RPM) diagram using the

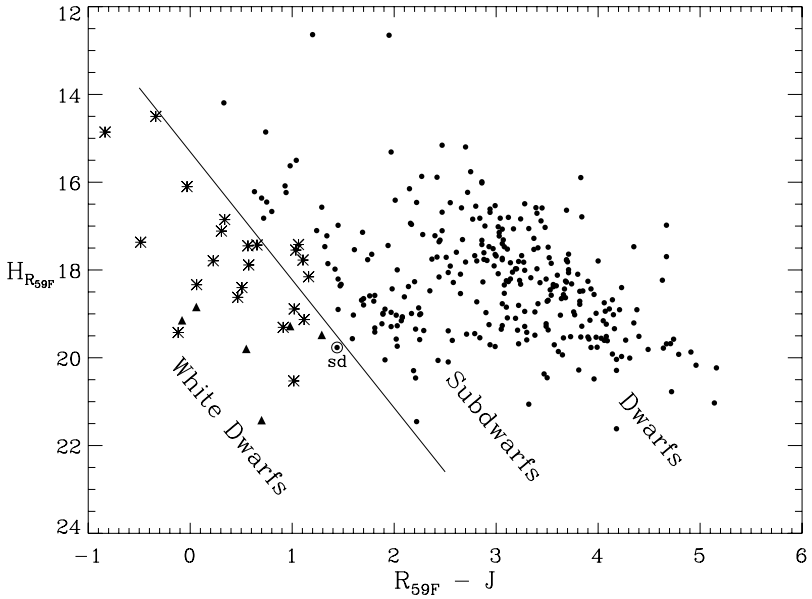

Figure 1. Reduced proper motion diagram used to select WD candidates for spectroscopic follow-up. Plotted are the 306 new high proper motion objects from Subasavage et al. (2005a, 2005b) for which both R_{59F} and J magnitudes were available. The line is a somewhat arbitrary boundary between the WDs (below) and the subdwarfs (just above). The main-sequence dwarfs fall above and to the right of the subdwarfs, although there is significant overlap. Asterisks indicate the 22 new WDs reported here. The six filled triangles in the WD region are confirmed WDs from the SCR survey and were published in Subasavage et al. (2007). The encircled point labeled "sd" is a confirmed subdwarf contaminant in the WD region.

$R_{59F} - J$ color was generated (see Figure 1). RPM (in this case, designated by $H_{R_{59F}}$ because the R_{59F} magnitude was used) is a quantity similar to absolute magnitude and is defined by

$$H_{R_{59F}} = R_{59F} + 5 + 5\log(\mu), \quad (1)$$

where μ is proper motion. It serves to relate two observed quantities, apparent magnitude and proper motion, to two intrinsic quantities, luminosity (absolute magnitude) and tangential velocity. The advantage of using the $R_{59F} - J$ color is that all SCR detections have an R_{59F} magnitude (defined by the survey). Given that WDs are relatively blue, the likelihood of registering a near-IR magnitude in the 2MASS database is greatest at J because its limiting magnitude is ∼1.0 mag fainter than K_S. Also, this color incorporates both optical plate and near-IR magnitudes that minimize the intrinsic uncertainties with plate magnitudes (e.g., nonlinearity). Both new SCR discoveries and known recoveries fell within the WD region of the RPM diagram. Most of the known objects had already been classified as WDs by previous researchers. Yet, a significant number of known high proper motion (HPM) objects within this region were not classified as WDs. It is likely that they escaped identification because of the poor plate magnitudes previously available. For instance, all plate magnitudes fainter than $m_{pg} = 10.0$ in the classic Luyten Half-Second (LHS) Catalogue (Luyten 1979a) and the New Luyten Two-Tenths (NLTT) Catalogue (Luyten 1979b) are by-eye estimates determined by Luyten (1979a). Rigorous calibrations performed by the SSS team yield high-quality plate magnitudes that reveal a number of new, relatively bright, WDs.

As an additional constraint, especially for objects near the arbitrary boundary that delineates the subdwarfs and the WDs, a $J - K_S$ color shift was implemented. As is evident in Figure 2, this color is degenerate for WDs (i.e., there is no unique absolute magnitude for a given color) and is always less than 0.5 mag (for single WDs). In contrast, subdwarfs near the boundary typically have $J - K_S \sim 0.6$ or larger and thus there exists a significant color gap to distinguish between the two luminosity classes.

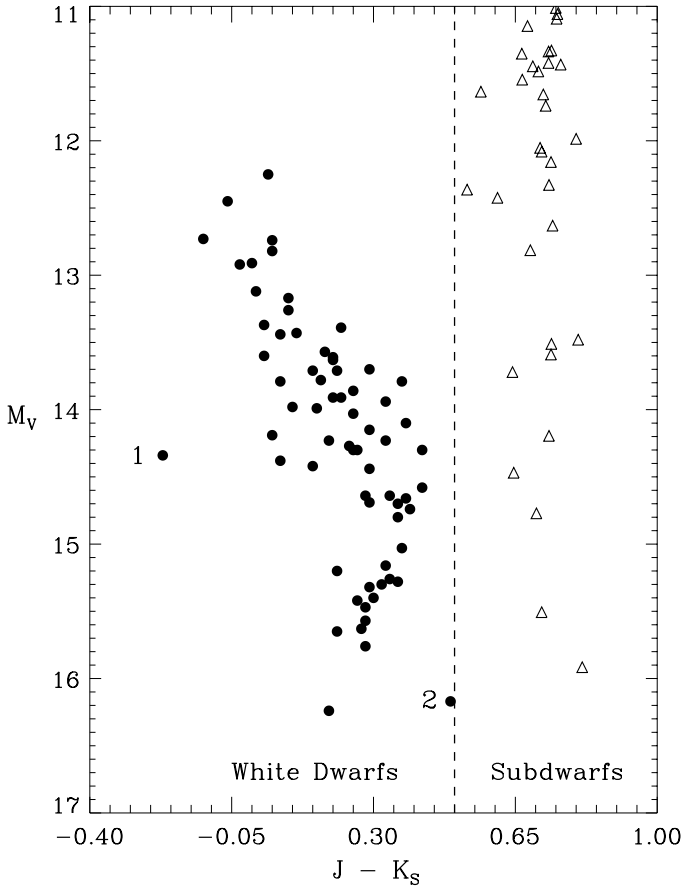

Figure 2. Plot of infrared $J - K_S$ color (transformed from the CIT system to the 2MASS system using the transformation equations of Carpenter 2001) vs. M_V for WDs within 25 pc (Bergeron et al. 2001) and late-type subdwarfs within 60 pc (W.-C. Jao 2008, private communication). Note how this particular color is less than 0.5 (vertical dashed line) over all M_V and is degenerate for the WDs. Numbered points are discussed in the text.

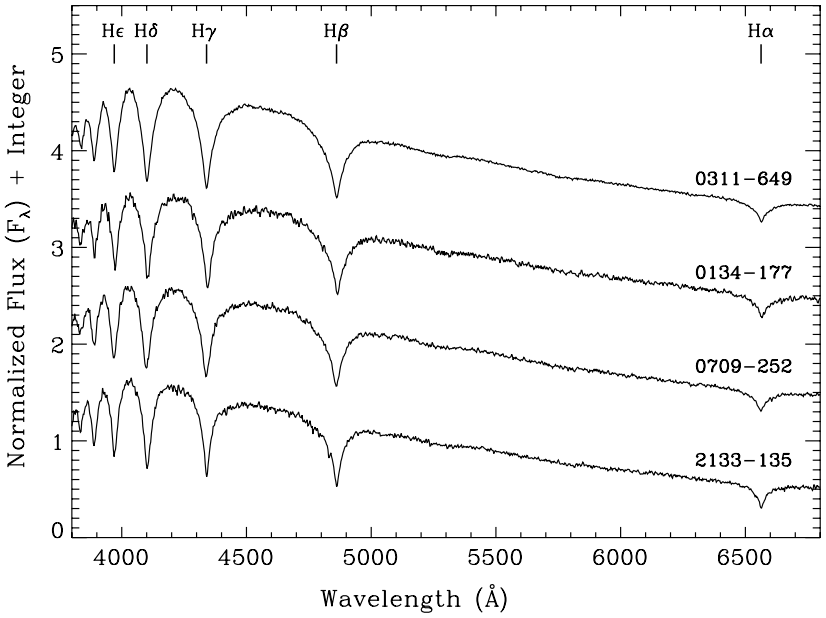

Figure 3. Spectral plots of the hot ($T_{\rm eff} \geqslant 10{,}000$ K) DA WDs from the new sample, plotted in descending $T_{\rm eff}$ as derived from the SED fits to the photometry. Spectra have been normalized at 5200 Å and offset by integer amounts. The inclusion of the spectrum of known object WD 2133−135 in this plot is discussed in Section 4.2.

Indeed, four new WDs were spectroscopically identified that are found in the subdwarf region of the RPM diagram. Two exceptional points in the WD region are: (1) WD 0548−001, which is a DQ WD (discussed in Dufour et al. 2005) that has a magnetic field of ∼10 MG (Kawka et al. 2007); (2) WD 2251−070, which is a DZ WD (discussed in Dufour et al. 2007) that is heavily line blanketed (Wesemael et al. 1993, Figure 11).

Before the candidates were targeted for spectroscopic follow-up observations, the basic linear plate relation of Oppenheimer et al. (2001) was used to estimate distances to candidates, assuming they were WDs. Only those candidates whose distance estimates were within ∼30 pc were selected for spectroscopic observations (this step was omitted from the procedures resulting in the new WD discoveries presented in Subasavage et al. 2007, hereafter referred to as Paper XIX). This constraint favored cooler, nearby stars so that even though the sample size of new systems presented here is smaller than that of Paper XIX (21 versus 33), more systems are estimated to be within 25 pc (12 versus 8). A total of 21 new WD systems (containing 22 WDs) were spectroscopically confirmed and are hereafter referred to as the "new sample." Optical photometry observations were obtained to improve distance estimates (discussed in Section 4.1).

Eleven known WDs without trigonometric parallaxes (hereafter referred to as the "known sample") were also targeted for optical photometry observations to improve their distance estimates. The known sample includes nine objects that previous authors predicted to be nearby (i.e., Aannestad et al. 1993; Holberg et al. 2002, 2008; Kawka et al. 2004, 2007; Pauli et al. 2006; Vennes & Kawka 2003) as well as two objects found via RPM that were known WDs but whose distances had not yet been estimated.

3. DATA AND OBSERVATIONS

3.1. Astrometry and Nomenclature

In keeping with the traditional naming convention for WDs, which uses the object's epoch 1950 equinox 1950 coordinates, 2MASS coordinates (when available, otherwise SSS coordinates were used) for the new systems presented here were extracted and adjusted for proper motion from the epoch of observation to epoch 2000 equinox 2000. The coordinates were then precessed to equinox 1950 using the IRAF task *precess* and again adjusted for proper motion (opposite in direction) to yield epoch 1950 equinox 1950 coordinates.

Proper motions for both the new and known samples were taken primarily from the SCR proper motion survey, but in a few cases from elsewhere in the literature. The appendix contains the proper motions used for coordinate adjustment, as well as J2000.0 coordinates and alternative names.

3.2. Spectroscopy

Spectroscopic observations were taken during two runs in 2006 May and December at the Cerro Tololo Inter-American Observatory (CTIO) 1.5 m telescope as part of the Small and Moderate Aperture Research Telescope System (SMARTS) Consortium. The Ritchey–Chrétien spectrograph and Loral 1200 × 800 CCD detector were used with grating 09 (in first order), providing 8.6 Å resolution and wavelength coverage from 3500 to 6900 Å. A slit width of 6″ was used and prevented the preferential light loss, at either the blue or the red end, encountered in the data presented in Paper XIX. Observations consisted of two exposures (typically 20–30 min each) to permit cosmic-ray rejection, followed by a comparison with the HeAr lamp exposure to calibrate wavelength for each object. Bias subtraction, dome/sky flat-fielding, and extraction of spectra were performed using standard IRAF packages.

Spectroscopic flux standards (two or three) were observed each night to calibrate the response of the CCD across the dispersion axis. However, because the selected flux standards are bright, neutral density filters of either 2.5 or 5.0 mag extinction were used. Thus, the resulting science spectra are relatively flux calibrated (i.e., the slopes are correct) but not on an absolute flux scale (i.e., erg cm^{-2} s^{-1} Å^{-1}). All spectra are normalized at 5200 Å for the sake of plotting.

Spectra for the new DA WDs with $T_{\rm eff} \geqslant 10{,}000$ K are plotted in Figure 3, while spectra for new DA WDs with

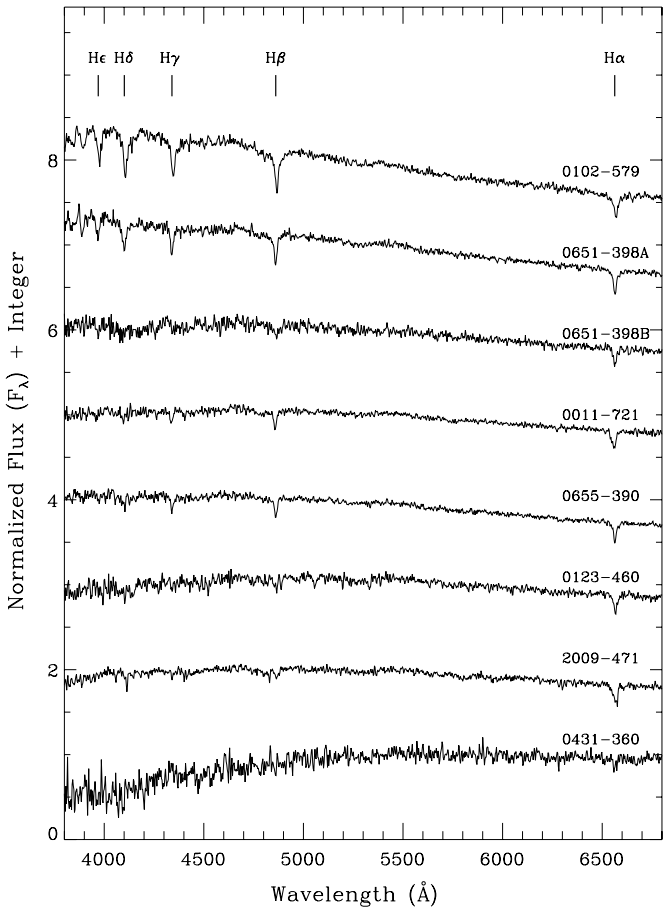

Figure 4. Spectral plots of cool ($T_{\rm eff}$ < 10,000 K) DA WDs from the new sample, plotted in descending $T_{\rm eff}$ as derived from the SED fits to the photometry. Spectra have been normalized at 5200 Å and offset by integer amounts. The asymmetry in the Hα feature in the spectrum of WD 2009−471 is the result of a cosmic ray landing just redward of Hα that could not be reliably removed.

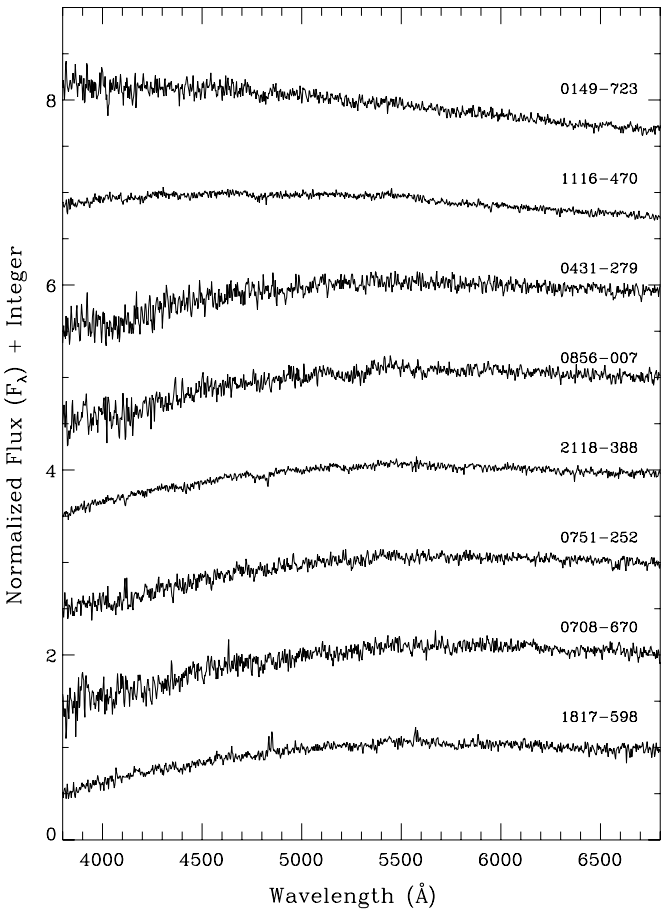

Figure 5. Spectral plots of featureless DC WDs from the new sample, plotted in descending $T_{\rm eff}$ as derived from the SED fits to the photometry. Spectra have been normalized at 5200 Å and offset by integer amounts.

$T_{\rm eff}$ < 10,000 K are plotted in Figure 4. Spectra for the new featureless DC WDs are plotted in Figure 5. Spectra, as well as model fits, for two new calcium-rich DZs, the hottest DA, and a helium-rich DB are shown in Figures 6 and 7 and are described in Section 4.1.

3.3. Photometry

Optical Johnson–Kron–Cousins *VRI*[6] photometry for the new and known WDs was obtained at the CTIO 0.9 m telescope during several observing runs from 2006 January through 2008 March as part of the SMARTS Consortium. The 2048 × 2046 Tektronix CCD camera was used with the Tex 2 *VRI* filter set. Standard stars from Graham (1982) and Landolt (1992, 2007) were taken nightly through a range of airmasses to calibrate fluxes to the Johnson–Kron–Cousins system and to calculate extinction corrections. Bias subtraction and flat-fielding (using calibration frames taken nightly) were performed using standard IRAF packages. When possible, an aperture of 14″ in diameter (consistent with Landolt 1992) was used to determine stellar flux. If cosmic rays fell within this aperture, they were removed before flux extraction. In cases of crowded fields or nearby companions, aperture corrections were applied and ranged from 4″ to 12″ in diameter using the largest aperture possible without including contamination from neighboring sources. Uncertainties in the optical photometry are ±0.03 mag in each band and incorporate both internal (night-to-night variations) and external (fits to the standard stars) uncertainties.[7] The final optical magnitudes are listed in Table 1, as well as the number of nights each object was observed.

4. ANALYSIS

4.1. Modeling of Physical Parameters

A detailed description of the model atmospheres used to model the WDs can be found in Paper XIX and references within. Briefly, the optical *VRI* and 2MASS near-IR JHK_S magnitudes are converted into observed fluxes and compared to the resulting spectral energy distributions (SEDs) predicted by the model atmosphere calculations. The observed flux, f_λ^m, is related to the model flux by the equation

$$f_\lambda^m = 4\pi(R/D)^2 H_\lambda^m, \quad (2)$$

where R/D is the ratio of the radius of the star to its distance from Earth, and H_λ^m is the Eddington flux (dependent on $T_{\rm eff}$, $\log g$, and atmospheric composition), properly averaged over the corresponding filter bandpass. We consider only $T_{\rm eff}$ and the solid angle $[\pi(R/D)^2]$ to be free parameters, and the uncertainties of both parameters are obtained directly from the covariance matrix of the fit. In this study, we simply assume a

[6] The central wavelengths for V_J, $R_{\rm KC}$, and $I_{\rm KC}$ are 5475, 6425, and 8075 Å, respectively.

[7] A complete discussion of the error analysis can be found in Henry et al. (2004).

Table 1
Optical and Infrared Photometry, and Derived Parameters for New and Known WDs

WD name	V_J	R_{KC}	I_{KC}	No. of obs.	J	σ_J	H	σ_H	K_S	σ_{K_S}	$T_{\rm eff}$ (K)	Comp.	Dist. (pc)	Spec. type	Notes
New spectroscopically confirmed WDs															
0011−721 ...	15.17	14.87	14.55	3	14.21	0.03	13.97	0.04	13.92	0.05	6439 ± 152	H	17.8 ± 2.9	DA8.0	a
0102−579 ...	16.35	16.17	15.98	2	15.67	0.07	15.57	0.16	15.76	Null	7866 ± 375	H	44.4 ± 7.5	DA6.5	b
0123−460 ...	16.30	15.94	15.57	3	15.11	0.04	14.84	0.06	14.91	0.10	5898 ± 161	H	24.9 ± 4.1	DA8.5	a
0134−177 ...	15.19	15.22	15.17	3	15.34	0.04	15.26	0.07	15.20	0.14	11329 ± 560	H	47.7 ± 8.4	DA4.5	c
0149−723 ...	16.33	16.10	15.86	2	15.65	0.05	15.64	0.12	15.42	0.18	6972 ± 298	He	36.2 ± 5.8	DC	
0311−649 ...	13.27	13.34	13.36	2	13.45	0.02	13.46	0.03	13.57	0.05	11945 ± 557	H	21.0 ± 3.7	DA4.0	d
0431−360 ...	17.03	16.55	16.08	2	15.48	0.06	15.17	0.08	15.23	0.18	5153 ± 154	H	25.2 ± 4.1	DA10.0	a
0431−279 ...	16.80	16.34	15.89	2	15.37	0.05	15.11	0.07	14.92	0.12	5330 ± 146	H	24.7 ± 4.0	DC	
0620−402 ...	16.20	15.89	15.60	2	15.27	0.04	15.13	0.09	15.24	0.17	5919 ± 278	He(+Ca)	25.3 ± 4.0	DZ	
0651−398A ...	15.46	15.23	14.98	2	14.71	0.04	14.55	0.05	14.49	0.11	7222 ± 219	H	25.1 ± 4.3	DA7.0	e
0651−398B ...	16.07	15.76	15.44	2	15.10	0.05	14.90	0.08	14.71	0.13	6450 ± 220	H	26.9 ± 4.5	DA8.0	a
0655−390 ...	15.11	14.81	14.48	3	14.15	0.03	13.88	0.04	13.89	0.07	6415 ± 162	H	17.2 ± 2.8	DA8.0	a
0708−670 ...	16.22	15.72	15.21	3	14.71	0.03	14.65	0.05	14.47	0.07	5108 ± 74	He	17.5 ± 2.7	DC	
0709−252 ...	14.38	14.36	14.34	2	14.39	0.03	14.39	0.04	14.49	0.09	10708 ± 356	H	30.5 ± 5.3	DA4.5	f
0751−252 ...	16.27	15.78	15.31	4	14.75	0.03	14.47	0.03	14.30	0.09	5159 ± 107	H	17.8 ± 2.9	DC	g
0816−310 ...	15.43	15.21	15.05	3	14.92	0.04	14.73	0.07	14.83	0.12	6631 ± 345	He(+Ca)	23.8 ± 3.8	DZ	
0856−007 ...	16.33	15.85	15.39	3	14.83	0.04	14.58	0.05	14.69	0.13	5309 ± 126	H	19.3 ± 3.2	DC	
1116−470 ...	15.52	15.20	14.86	3	14.45	0.03	14.37	0.06	14.35	0.09	5856 ± 140	He	17.9 ± 2.8	DC	
1817−598 ...	16.85	16.30	15.80	3	15.20	0.05	15.01	0.10	14.91	0.14	4960 ± 145	H	20.9 ± 3.4	DC	
1916−362 ...	13.60	13.69	13.77	2	14.10	0.03	14.22	0.04	14.21	0.07	24105 ± 8797	He	41.7 ± 7.7	DB	h
2009−471 ...	16.53	16.16	15.79	2	15.38	0.05	15.00	0.05	15.08	0.12	5827 ± 162	H	27.0 ± 4.5	DA8.5	a
2118−388 ...	16.55	16.09	15.65	2	15.16	0.04	14.92	0.07	15.05	0.12	5244 ± 102	He	22.0 ± 3.5	DC	
Known WDs (without trigonometric parallaxes)															
0233−242	15.94	15.43	14.93	3	14.45	0.03	14.34	0.05	14.12	0.07	5093 ± 78	He	15.3 ± 2.4	DC	i
0707−320 ...	15.61	15.57	15.49	2	15.49	0.06	15.43	0.11	15.38	0.20	9900 ± 440	H	47.8 ± 8.2	DA5.0	
1223−659 ...	14.02	13.82	13.62	3	13.33	0.04	13.26	0.06	13.30	0.06	7690 ± 220	H	14.5 ± 2.5	DA6.5	j
1241−798 ...	16.18	15.80	15.45	3	15.03	0.05	14.83	0.07	14.60	0.12	5618 ± 143	He	22.1 ± 3.5	DC/DQ	
2007−219 ...	14.40	14.33	14.25	3	14.20	0.02	14.20	0.04	14.26	0.08	9556 ± 242	H	25.7 ± 4.4	DA5.5	k
2133−135 ...	13.68	13.63	13.55	3	13.60	0.03	13.58	0.04	13.69	0.06	10182 ± 281	H	20.4 ± 3.5	DA5.0	l
2159−754 ...	15.04	14.92	14.80	2	14.72	0.04	14.67	0.07	14.55	0.10	8944 ± 289	H	30.5 ± 5.3	DA5.5	m
2216−657 ...	14.55	14.47	14.41	2	14.54	0.04	14.50	0.06	14.53	0.09	10611 ± 567	He	30.1 ± 5.1	DZ	n
2306−220 ...	13.75	13.83	13.89	2	14.13	0.03	14.18	0.05	14.33	0.07	16285 ± 1273	H	33.3 ± 6.1	DA3.0	o
2336−079 ...	13.28	13.27	13.24	4	13.34	0.03	13.34	0.02	13.35	0.03	10946 ± 304	H	18.9 ± 3.3	DA4.5	p
2351−335 ...	14.52	14.38	14.19	2	13.99	0.11	13.86	0.25	13.73	0.11	8068 ± 401	H	20.1 ± 3.5	DA6.0	q

Notes.
[a] Too cool for a reliable spectroscopic fit (i.e., minimal Balmer line absorption).
[b] Spectral fit yielded $T_{\rm eff} = 8228 \pm 138$ K and $\log g = 8.19 \pm 0.12$. Common proper motion companion to NLTT 3566 (see Section 4.2).
[c] Spectral fit yielded $T_{\rm eff} = 11613 \pm 192$ K and $\log g = 8.14 \pm 0.06$.
[d] Spectral fit yielded $T_{\rm eff} = 12632 \pm 300$ K and $\log g = 7.63 \pm 0.06$ (see Section 4.2).
[e] Spectral fit yielded $T_{\rm eff} = 7214 \pm 135$ K and $\log g = 7.68 \pm 0.19$. Common proper motion companion to WD 0651−398B (see Section 4.2).
[f] Spectral fit yielded $T_{\rm eff} = 11208 \pm 180$ K and $\log g = 8.12 \pm 0.06$.
[g] Common proper motion companion to LTT 2976 (see Section 4.2).
[h] Spectral fit yielded $T_{\rm eff} = 27830 \pm 1050$ K and $\log g = 7.97 \pm 0.07$ (see Section 4.2 and Figure 7).
[i] Vennes & Kawka (2003) estimate a distance of 15 pc.
[j] Holberg et al. (2002) estimate a distance of 10.79 pc. Holberg et al. (2008) estimate a distance of 12.05 pc.
[k] Holberg et al. (2002) estimate a distance of 18.22 pc.
[l] Spectral fit yielded $T_{\rm eff} = 10357 \pm 158$ K and $\log g = 7.99 \pm 0.07$. Pauli et al. (2006) estimate a distance of 23.3 pc (see Section 4.2).
[m] Kawka et al. (2007) estimate a distance of 14 pc. Holberg et al. (2008) estimate a distance of 14.24 pc.
[n] Aannestad et al. (1993) estimate a distance of 28 pc.
[o] Kawka et al. (2004) estimate a distance of 33 pc.
[p] Holberg et al. (2002) estimate a distance of 15.6 pc. Holberg et al. (2008) estimate a distance of 17.45 pc.
[q] Holberg et al. (2002) estimate a distance of 12.41 pc.

value of $\log g = 8.0$ for each star. As discussed in Bergeron et al. (1997, 2001), the main atmospheric constituent—hydrogen or helium—is determined by comparing the fits obtained with both compositions, or by the presence of Hα in the optical spectra. The derived values for $T_{\rm eff}$ for each object are listed in Table 1. For the two new DZ stars, spectroscopic modeling of metal lines as well as photometry was used to constrain $T_{\rm eff}$ (see below). Also listed are the spectral types for each object determined based on their spectral features. The DAs have been assigned a half-integer temperature index as defined by McCook & Sion (1999), where the temperature index equals $50{,}400/T_{\rm eff}$.

Our grids of model atmospheres and synthetic spectra for DA and DB stars are described respectively in Liebert et al. (2005) and Beauchamp et al. (1996). The atmospheric parameters—

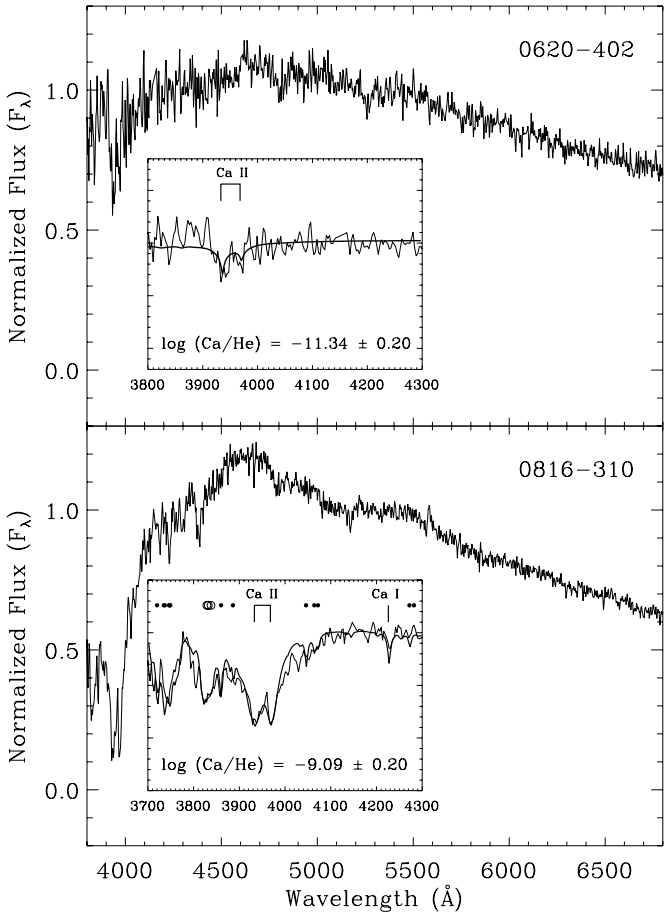

Figure 6. Spectral plots of the two DZ WDs from the new sample. The inset plots display the spectra (thin lines) in the regions to which the models (thick lines) were fit. Spectroscopic best-fit physical parameters are listed below. Prominent lines from Ca (vertical lines), Mg (open circles), and Fe (filled circles) are labeled. Both modeled fits incorporated slight hydrogen abundance of log (H/He) = −3 (see Section 4.1).

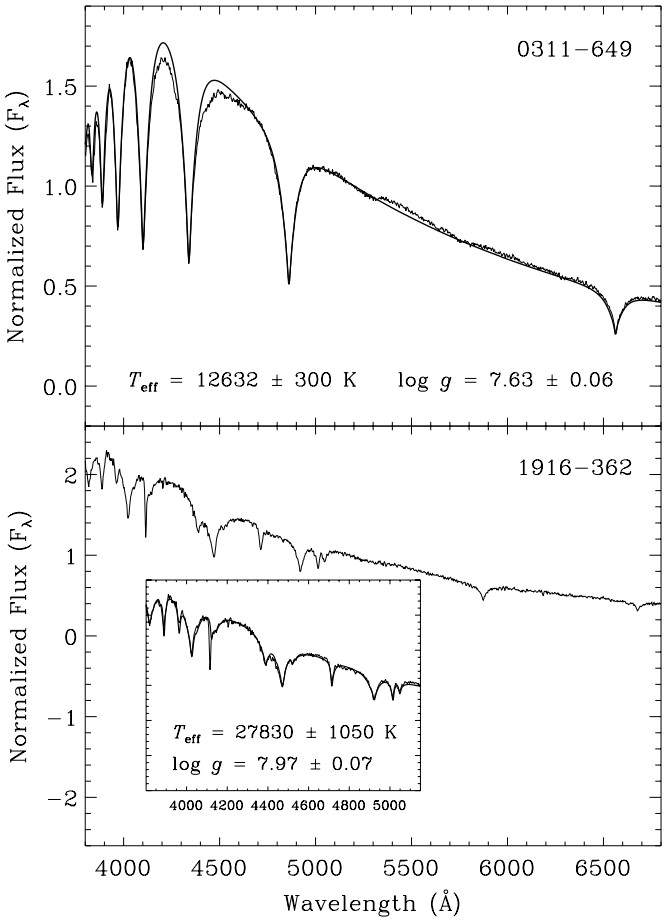

Figure 7. Top: spectral plot of the DA (hydrogen-rich) WD 0311−649 with the model fit (thick line) overplotted. Spectroscopic best-fit physical parameters are listed below. Bottom: spectral plot of the DB (helium-rich) WD 1916−362. The inset plot displays the spectrum (thin line) in the region to which the model (thick line) was fit. Spectroscopic best-fit physical parameters are listed below. Note that the sharp absorption feature at ∼4100 Å is an artifact produced by a cosmic ray that could not be reliably removed because of its proximity to a true spectral feature.

$T_{\rm eff}$, log g (and hydrogen abundance for the DB stars)—are determined from the optical spectra using the so-called spectroscopic technique (see, e.g., Bergeron et al. 1992), which relies on a detailed comparison between synthetic and observed normalized line profiles. The model spectra (convolved with a Gaussian instrumental profile) and the optical spectrum are first normalized to a continuum set to unity. The calculation of χ^2 is then carried out in terms of these normalized line profiles only, and the best-fitting solution is obtained using the nonlinear least-squares method of Levenberg–Marquardt (Press et al. 1992), which is based on a steepest descent method. Spectroscopically derived values of $T_{\rm eff}$ and log g are given in the footnotes of Table 1 for the DA and DB stars.

For the DZ stars' spectra in Figure 6, we rely on the procedure outlined in Dufour et al. (2007). We obtain a first estimate of the atmospheric parameters by fitting the photometric SED with an assumed value of the metal abundances (assuming solar abundance ratios). We then fit the optical spectrum to measure the metal abundances, and use these values to improve our atmospheric parameters from the photometric SED. This procedure is iterated until a self-consistent photometric and spectroscopic solution is achieved. In the cases of the two DZ stars presented here, slight abundance of hydrogen was included [log(H/He) = −3] in the modeled fits. As shown in Dufour et al. (2007), the Ca line widths and depths are affected by the presence of hydrogen even if the abundance is not significant enough to produce spectral signatures. Our spectra were best fit with the inclusion of hydrogen. The values of $T_{\rm eff}$ listed in Table 1 for the new DZ stars were derived using this additional spectroscopic modeling constraint (i.e., "He(+Ca)" in the composition column), whereas the known DZ (WD 2216−657) was modeled using only photometry assuming a pure He atmosphere (i.e., "He" in the composition column).

Once the effective temperature and the atmospheric composition were determined, we calculated the absolute visual magnitude using a procedure identical to that outlined in Paper XIX (i.e., the new photometric calibration of Holberg et al. 2006, combined with evolutionary models[8]). We then compared the absolute magnitude to the apparent V magnitude observed to derive a distance estimate for each star (reported in Table 1). Errors on the distance estimates incorporate the errors of the photometry values as well as an error of 0.25 dex in log g, which is the measured dispersion of the observed distribution using spectroscopic determinations (see Figure 9 of Bergeron et al. 1992).

[8] See http://www.astro.umontreal.ca/∼bergeron/CoolingModels/.

4.2. Comments on Individual Systems

WD 0102–579: a new HPM object discovered during the SCR proper motion survey ($\mu = 0\farcs239$ yr^{-1} at position angle 91°.1, Finch et al. 2007). It is likely a common proper motion companion to a previously known HPM object, the red dwarf NLTT 3566 ($\mu = 0\farcs257$ yr^{-1} at position angle 87°.5), separated by 110″.6 at position angle 206°.6. The *Hipparcos* parallax for NLTT 3566 is 19.51 ± 3.13 mas (distance = 51.3 ± 9.8 pc, van Leeuwen 2007), entirely consistent with our distance estimate for the WD of 44.4 ± 7.5 pc.

WD 0311–649: the hottest DA WD in the new sample ($T_{\rm eff}$ = 11,945 ± 557 K). The Balmer lines of our high signal-to-noise (S/N) spectrum are best fit to a spectral fitting model with $T_{\rm eff}$ = 12,632 ± 300 K and log g = 7.63 ± 0.06 (see Figure 7), significantly less than the assumed value of log g = 8.0 in the photometric analysis. This would imply that the object is low mass ($M = 0.42 \pm 0.03\ M_{\odot}$) and more luminous thereby making it more distant (∼28 pc). Given the age of our Galaxy, the lowest-mass WD that could have formed is ∼0.47 $M_{\odot}$ (Iben & Renzini 1984). If the mass is correct, it is extremely unlikely that this object formed through single-star evolution and thus is likely a multiple system. Trigonometric parallax measurements are underway to confirm the luminosity and hence the mass via our Cerro Tololo Inter-American Observatory Parllax Investigation (CTIOPI, Jao et al. 2005; Costa et al. 2005, 2006; Henry et al. 2006).

WD 0620–402: a new DZ WD whose modeled physical parameters place this object in a lower temperature realm where high atmospheric pressure effects exist that are not included in the Ca-rich (DZ) models described in Section 4.1. Thus, the model fit is likely inaccurate for this object, so that the physical parameters derived are not well constrained (especially given the low S/N of the spectrum, see Figure 6).

WD 0651–398AB: a widely separated (87″.2 at position angle 317°.4) HPM double degenerate system discovered during the SCR proper motion survey. The A component ($\mu = 0\farcs229$ yr^{-1} at position angle 344°.7) has $T_{\rm eff}$ = 7222 ± 219 K and the B component ($\mu = 0\farcs227$ yr^{-1} at position angle 344°.4) has $T_{\rm eff}$ = 6450 ± 220 K. A third object, WT 204, is separated by 59′.3 at position angle 67°.2 and has a similar proper motion of 0″.213 yr^{-1} at position angle 341°.9. We have obtained spectra and optical photometry, which indicate a spectral type of M3.0V and V_J = 13.17, $R_{\rm KC}$ = 12.03, $I_{\rm KC}$ = 10.60. Using the main-sequence distance relations of Henry et al. (2004), we obtain a distance estimate of 19.8 ± 3.1 pc, which is entirely consistent with the distance estimates to the A and B components, 25.1 ± 4.3 pc and 26.9 ± 4.5 pc, respectively. While highly unlikely that this is a bound system (the third component's separation is ∼90,000 AU), it is possible that they are part of a moving group.

WD 0751–252: a new HPM object discovered during the SCR proper motion survey ($\mu = 0\farcs426$ yr^{-1} at position angle 300°.2, Subasavage et al. 2005b). Its proper motion is similar to a previously known HPM object, LTT 2976 ($\mu = 0\farcs361$ yr^{-1} at position angle 303°.8). The distance estimate for the WD (17.8 ± 2.9 pc) is consistent with the *Hipparcos* parallax of 51.53 ± 1.46 mas (distance = 19.41 ± 0.57 pc, van Leeuwen 2007) for LTT 2976. Thus, these two objects likely form a system with a separation of 6′.6 (∼8000 AU) at position angle 208°.9.

WD 0816–310: a new DZ WD whose spectrum has been reliably reproduced using the methods appropriate for DZs described in Section 4.1 (see Figure 6). The inset plot extends down to 3700 Å (rather than 3800 Å for all other spectral plots) to illustrate the validity of assuming solar abundance ratios (at least for Ca, Mg, and Fe) given the quality of the fit.

WD 1916–362: the only DB WD in the new sample. The photometric temperature ($T_{\rm eff}$ = 24,105 ± 8797 K) agrees reasonably well with the spectroscopic temperature ($T_{\rm eff}$ = 27,830 ± 1050 K) assuming a pure helium composition given that no hydrogen features are visible in the spectrum. At these temperatures, trace amounts of hydrogen may be present without showing any spectral signatures and would serve to reduce the spectroscopic temperature. In fact, hydrogen would go unnoticed spectroscopically until at least log (H/He) = −3.5 was included. If we assume a log (H/He) = −4.5 (i.e., not spectrally visible), we obtain a spectroscopic solution with $T_{\rm eff}$ = 25,800 K, slightly more consistent with the photometric temperature. It is possible that trace amounts of hydrogen are present, however, without additional information (i.e., a trigonometric parallax); we have chosen to adopt the spectroscopic result assuming a pure helium composition.

We note that the photometric temperature is far more uncertain. The optical photometry used to fit the SED is rather insensitive to effective temperature because the magnitudes fall largely on the Rayleigh–Jeans tail of the SED for such a hot object. Therefore, the spectroscopically determined effective temperature is significantly better constrained (spectrum and fit are plotted in Figure 7).

WD 2133–135: a DA WD that was uncovered during our sift of the SSS database. It is also included in Pauli et al. (2006) (labeled HE 2133−1332 in that work), in which they analyzed spectra of 398 DA WDs to determine kinematic properties of the sample as part of the SN Ia Progenitor surveY (SPY). The authors state that their sample was generated from databases of known WDs; however, we performed a thorough search for a previous spectroscopic confirmation of this object's WD status and were unsuccessful.[9] We have confirmed that this object was selected to be observed by the SPY project using data taken from the Hamburg/ESO (HE) survey in which there was no previous confirmation spectrum but rather a high confidence in this object's luminosity class (R. Napiwotzki 2008, private communication). Thus, Pauli et al. (2006) is the first publication to confirm this object's WD status (hence, it is a member of the known sample) yet this publication is the first to present a confirmation spectrum (see Figure 3). The authors estimate a spectroscopic distance of 23.3 pc, consistent with our distance estimate of 20.4 ± 3.5 pc.

WD 2159–754: a known DA WD that has been analyzed spectroscopically by Kawka et al. (2007) for which they determine the spectroscopic $T_{\rm eff}$ = 9040 ± 80 K, moderately consistent with our photometric $T_{\rm eff}$ = 9556 ± 242 K. In addition, they conclude that this object has a large surface gravity (log $g = 8.95 \pm 0.12$) and hence a large mass ($1.17 \pm 0.04\ M_{\odot}$). Thus, their estimated distance (14 pc) is significantly closer than our estimated distance (30.5 ± 5.3 pc) based on an assumed log g = 8.0. Trigonometric parallax measurements are underway to confirm its luminosity and hence its mass.

[9] Resources searched include the WD database of McCook & Sion (1999) (the current Web-based catalog can be found at http://heasarc.nasa.gov/W3Browse/all/mcksion.html) as well as a previous WD publication using data from the Hamburg/ESO (HE) survey (i.e., Christlieb et al. 2001).

Table 2
Distance Estimate Statistics for New and Known WD Systems[a]

Proper motion (arcsec yr^{-1})	$d \leqslant 10$ (pc)	$10 < d \leqslant 25$ (pc)	$d > 25$ (pc)
$\mu \geqslant 1.0 \ldots$	1 + 0	6 + 0	1 + 0
$1.0 > \mu \geqslant 0.8 \ldots$	0 + 0	0 + 1	0 + 0
$0.8 > \mu \geqslant 0.6 \ldots$	0 + 0	2 + 2	2 + 1
$0.6 > \mu \geqslant 0.4 \ldots$	0 + 0	6 + 4	11 + 2
$0.4 > \mu \geqslant 0.2 \ldots$	0 + 0	4 + 7	20 + 11
$0.2 > \mu \geqslant 0.0 \ldots$	0 + 0	1 + 4	2 + 0
Total	1 + 0	19 + 18	36 + 14

Note. [a] The first number is from Paper XIX, and the second number is from this paper.

5. DISCUSSION

We continue to fill in the nearby WD sample with the discovery of 21 new WD systems brighter than $V \sim 17$. While the sample size is smaller than the number of new WDs presented in Paper XIX, the number of new systems estimated to be within 25 pc is larger (eight reported in Paper XIX versus 12 reported here for a total of 20 new WDs), due largely to the revised criteria set for candidates to be targeted for follow-up spectroscopic observations (see Section 2). In addition, of the known samples evaluated in this effort, a total of 18 WDs are estimated to be within 25 pc (12 reported in Paper XIX and six reported here). Combining the new and known samples from both publications, we have found a total of 38 WDs estimated to be within 25 pc—a volume that currently contains 110 WD systems disregarding any quality constraints on the parallaxes.[10] Trigonometric parallax determinations are underway to confirm membership to the 25 pc sample but should the distance estimates prove accurate, the local sample of WDs will be increased by 34%. Once these nearby WDs are confirmed, focused efforts can yield crucial WD masses and permit companionship assessments.

To ensure a reliable sample, we have begun to adopt the quality constraint that the trigonometric parallax error cannot be greater than 10% of the parallax. Given the precision of ground-based trigonometric parallaxes (∼2.0 mas or better), this constraint is entirely reasonable (even for a system at the 25 pc horizon, the 10% constraint amounts to an error of 4.0 mas). With the constraint in place, 13 systems (five in the north and eight in the south) are eliminated from the known 25 pc WD sample (now with a total of 97 systems). To better constrain their distances, we are currently measuring trigonometric parallaxes for seven of these systems in the southern hemisphere (one system, WD 1043−188 is too close to a companion whose brightness exceeds the bright limit of 0.9 m at CTIO). We would encourage northern hemisphere parallax programs to do the same for the five systems in the north (WD 0644+025, WD 0955+247, WD 1309+853, WD 1919+145, and WD 2117+539).

If we separate new and known samples from Paper XIX and this work by proper motion, we see that the majority of added WD neighbors estimated to be within 25 pc is found at lower proper motions. Table 2 breaks down this complete sample into proper motion bins of 0.″2 yr^{-1} below 1.″0 yr^{-1} (the first value in each column corresponds to the systems presented in Paper XIX while the second value corresponds to those systems reported here). A quick summation shows that the number of systems with $\mu \geqslant 0.''6$ yr^{-1} (12) is dwarfed by the number of systems with $\mu < 0.''6$ yr^{-1} (26), including five that have $\mu < 0.''2$ yr^{-1} (of which, four have μ between 0.18 and 0.″2 yr^{-1}). These results support the notion that a significant number of nearby WDs may still be found at very low proper motions.

Other recent efforts have focused on the local WD population. In particular, Holberg et al. (2008) have targeted the 20 pc sample determined by trigonometric parallaxes as well as photometric/spectroscopic parallaxes. The authors estimate the local WD density based on the 13 pc WD sample using the assumption that the 13 pc sample is largely complete. Paper XIX contained two objects (WD 0821−669 and WD 1202−232) previously unknown to be nearby, whose distance estimates as well as unpublished trigonometric parallaxes (J. P. Subasavage et al. 2008, in preparation) placed them within 13 pc. These have been included by Holberg et al. (2008) in their updated estimate of the local WD density. Given that none of the new WD discoveries in this publication have distance estimates within 13 pc, the notion that the 13 pc WD sample is largely complete is supported. The sample of Holberg et al. (2008) includes five new WD discoveries from Paper XIX whose distance estimates lie within 20 pc (WD 0121−429, WD 0344+014, WD 0821−669, WD 2008−600, WD 2138−332) as well as one from this paper (WD 0751−252, see Section 4.2). The authors estimate that the 20 pc sample is ∼80% complete and that ∼33 ± 13 WDs remain to be discovered between 13 and 20 pc (again assuming the 13 pc sample is complete). Five systems reported here (not including WD 0751−252) are estimated to lie within 20 pc. Thus, we fill the incompleteness gap.

A star's mass is one of its most important characteristics that, when coupled with composition and luminosity, defines several fundamental properties of that star such as its internal structure, future evolution, and total lifetime. The same is true for WDs; however, only three WDs have measured astrometric mass determinations better than 5% (Sirius B, Procyon B, 40 Eri B and Provencal et al. 2002). The identification of WDs in binaries, in particular double-degenerate systems, may increase the number of accurate astrometric masses of WDs if the system were resolvable using high-precision astrometric techniques (e.g., speckle, adaptive optics, or interferometry via the *Hubble Space Telescope*'s Fine Guidance Sensors). Of course, the nearer the system is to the Sun, the greater its projected separation and more likely it is to be resolved, all else being equal. A sizable sample of accurate WD masses will help constrain and revise WD models, while comprehensive searches for companions in a volume-limited sample will allow an accurate multiplicity fraction to be determined.

We continue to measure trigonometric parallaxes with good precision from the ground (∼1.1 mas errors on average, J. P. Subasavage et al. 2008, in preparation) for the nearby WD sample as part of the CTIOPI program. In addition, nearly all WDs within 15 pc in the southern hemisphere (including those we have presented in Paper XIX and here) have been targeted for long-term astrometric monitoring in search of perturbations from unseen companions. This effort is an extension of the Astrometric Search for Planets Encircling Nearby Stars (ASPENS; Koerner et al. 2003) that target all red and WDs within 10 pc

[10] This sample of WDs was compiled using parallaxes, both for the WDs and for additional components if the WD is part of a multiple system, from the Yale Parallax Catalog (van Altena et al. 1995), *Hipparcos* (Perryman et al. 1997; van Leeuwen 2007), and other recent efforts involving trigonometric parallaxes (e.g., Smart et al. 2003; Gould & Chanamé 2004; Ducourant et al. 2007). A comprehensive list, including weighted mean parallaxes when multiple parallaxes are available for a system, can be found at http://www.DenseProject.com.

Table 3
Astrometry and Alternate Designations for New and Known WDs

WD name	R.A. (J2000.0)	Decl. (J2000.0)	PM (arcsec yr^{-1})	PA (deg)	Ref	Alternative names
New spectroscopically confirmed WDs						
0011−721 ...	00 13 49.91	−71 49 54.2	0.326	141.3	S	NLTT 681, LP 50-73
0102−579 ...	01 04 12.14	−57 42 48.6	0.239	091.1	S	SCR 0104−5742
0123−460 ...	01 25 18.03	−45 45 31.1	0.759	137.8	S	SCR 0125−4545
0134−177 ...	01 37 15.16	−17 27 22.6	0.319	189.3	S	NLTT 5424, LP 768-192
0149−723 ...	01 50 38.49	−72 07 16.7	0.334	223.9	S	SCR 0150−7207
0311−649 ...	03 12 25.68	−64 44 10.8	0.190	105.6	S	WT 106, LEHPM 1-3159
0431−360 ...	04 32 55.87	−35 57 28.9	0.301	084.1	S	LEHPM 2-1182
0431−279 ...	04 33 33.58	−27 53 24.8	0.403	092.4	S	NLTT 13532, LP 890-39, LEHPM 2-405
0620−402 ...	06 21 41.64	−40 16 18.7	0.379	166.0	S	LEHPM 2-505
0651−398A ...	06 53 30.21	−39 54 29.1	0.227	344.4	S	WT 202
0651−398B ...	06 53 35.34	−39 55 33.3	0.229	344.7	S	WT 201
0655−390 ...	06 57 05.90	−39 09 35.7	0.340	242.6	S	NLTT 17220, L 454-9, LTT 2692
0708−670 ...	07 08 52.28	−67 06 31.4	0.246	246.3	S	SCR 0708−6706
0709−252 ...	07 11 14.39	−25 18 15.0	0.223	334.4	S	SCR 0711−2518
0751−252 ...	07 53 56.61	−25 24 01.4	0.426	300.2	S	SCR 0753−2524
0816−310 ...	08 18 40.26	−31 10 20.3	0.842	162.6	S	SCR 0818−3110
0856−007 ...	08 59 12.91	−00 58 42.9	0.202	125.8	S	NLTT 20690, LP 606-32
1116−470 ...	11 18 27.20	−47 21 57.0	0.322	275.1	S	SCR 1118−4721
1817−598 ...	18 21 59.54	−59 51 48.5	0.365	194.9	S	SCR 1821−5951
1916−362 ...	19 20 02.83	−36 11 02.7	0.208	132.0	S	SCR 1920−3611
2009−471 ...	20 12 48.75	−46 59 02.5	0.244	136.3	S	WT 689
2118−388 ...	21 22 05.59	−38 38 34.7	0.186	113.5	S	SCR 2122−3838
Known WDs (without trigonometric parallaxes)						
0233−242 ...	02 35 21.80	−24 00 47.3	0.620	189.5	S	LHS 1421, NLTT 8435, LP 830-14
0707−320 ...	07 09 25.07	−32 05 07.3	0.551	338.2	L	LHS 1898, NLTT 17486, LP 896-18
1223−659 ...	12 26 42.02	−66 12 18.5	0.190	182.0	L	NLTT 30737, LP 104-2, GJ 2092
1241−798 ...	12 44 52.70	−80 09 27.8	0.578	306.3	L	LHS 2621, NLTT 31694, LP 38-80
2007−219 ...	20 10 17.51	−21 46 45.6	0.311	158.0	L	NLTT 48815, LP 870-43
2133−135 ...	21 36 16.38	−13 18 34.5	0.297	120.2	S	NLTT 51636, Ross 203, HE 2133-1332
2159−754 ...	22 04 20.84	−75 13 26.1	0.523	277.6	S	LHS 3752, NLTT 52728, LP 48-15
2216−657 ...	22 19 48.31	−65 29 17.6	0.660	160.1	L	LHS 3794, NLTT 53489, LP 119-34
2306−220 ...	23 08 40.78	−21 44 59.6	0.350	109.0	S	NLTT 55932, LP 877-69
2336−079 ...	23 38 50.74	−07 41 19.9	0.034	126.6	Su	GD 1212
2351−335 ...	23 54 01.14	−33 16 30.3	0.500	216.5	L	LHS 4040, NLTT 58330, LP 936-12

References: (L) Luyten (1979a, 1979b); (S) Subasavage et al. (2005a, 2005b); Finch et al. (2007), this work; (Su) J. Subasavage et al. (2008, in preparation).

in the southern hemisphere. Because of the spectral signatures of WDs (broad absorption lines or no lines at all), astrometry is currently the only practical method for detecting sub-stellar/planetary companions to WDs. Unlike radial velocity variations used to detect planetary systems, astrometric signatures are linearly related to the distance to the system (the farther the system, the smaller the astrometric signature). Thus, a careful evaluation of the nearest WDs provides the highest probability for detecting astrometric signatures of companions to WDs.

We wish to thank the referee of this manuscript for helpful comments that improved the clarity of this publication. The RECONS team at Georgia State University wishes to thank the NSF (grant AST 05-07711), NASA's Space Interferometry Mission, the Space Telescope Science Institute (grant HST-GO-10928.01-A), and GSU for their continued support in our study of nearby stars. We also thank the members of the SMARTS Consortium, who enable the operations of the small telescopes at CTIO where all of the data in this work were collected. J.P.S. is indebted to Wei-Chun Jao for the use of his photometry reduction pipeline. P.B. is a Cottrell Scholar of Research Corporation and would like to thank the NSERC Canada and the fund FQRNT (Québec) for their support. N.C.H. would like to thank colleagues in the Wide Field Astronomy Unit at Edinburgh for their efforts contributing to the SSS effort; particular thanks go to Mike Read, Sue Tritton, and Harvey MacGillivray. This work has made use of the SIMBAD, VizieR, and Aladin databases, operated at the CDS in Strasbourg, France. We have also used data products from the Two Micron All Sky Survey, which is a joint project of the University of Massachusetts and the Infrared Processing and Analysis Center, funded by NASA and NSF.

APPENDIX

In order to ensure correct cross-referencing of names for the new and known WD systems presented here, Table 3 lists additional names found in the literature. Objects for which there is an NLTT designation also have the corresponding L or LP designation found in the NLTT catalog. These L or LP names are listed here because the NLTT designations were not published in the original catalog, but rather are the record numbers in the electronic version of the catalog and have been adopted out of necessity.

REFERENCES

Aannestad, P. A., Kenyon, S. J., Hammond, G. L., & Sion, E. M. 1993, AJ, 105, 1033

Beauchamp, A., Wesemael, F., Bergeron, P., Liebert, J., & Saffer, R. A. 1996, in ASP Conf. Ser. 96, Hydrogen-Deficient Stars, ed. S. Jeffery, & U. Heber (San Francisco, CA: ASP), 295

Bergeron, P., Leggett, S. K., & Ruiz, M. T. 2001, ApJS, 133, 413

Bergeron, P., Ruiz, M. T., & Leggett, S. K. 1997, ApJS, 108, 339

Bergeron, P., Saffer, R. A., & Liebert, J. 1992, ApJ, 394, 228

Carpenter, J. M. 2001, AJ, 121, 2851

Christlieb, N., Wisotzki, L., Reimers, D., Homeier, D., Koester, D., & Heber, U. 2001, A&A, 366, 898

Costa, E., Méndez, R. A., Jao, W.-C., Henry, T. J., Subasavage, J. P., Brown, M. A., Ianna, P. A., & Bartlett, J. 2005, AJ, 130, 337

Costa, E., Méndez, R. A., Jao, W.-C., Henry, T. J., Subasavage, J. P., & Ianna, P. A. 2006, AJ, 132, 1234

Ducourant, C., Teixeira, R., Hambly, N. C., Oppenheimer, B. R., Hawkins, M. R. S., Rapaport, M., Modolo, J., & Lecampion, J. F. 2007, A&A, 470, 387

Dufour, P., Bergeron, P., & Fontaine, G. 2005, ApJ, 627, 404

Dufour, P., et al. 2007, ApJ, 663, 1291

Finch, C. T., Henry, T. J., Subasavage, J. P., Jao, W.-C., & Hambly, N. C. 2007, AJ, 133, 2898

Gliese, W., & Jahreiß, H. 1991, in The Astronomical Data Center CD-ROM: Selected Astronomical Catalogs 1, ed. L. E. Brotzmann, & S. E. Gesser (Greenbelt, MD: NASA/Astronomical Data Center, Goddard Space Flight Center)

Graham, J. A. 1982, PASP, 94, 244

Gould, A., & Chanamé, J. 2004, ApJS, 150, 455

Hambly, N. C., Henry, T. J., Subasavage, J. P., Brown, M. A., & Jao, W.-C. 2004, AJ, 128, 437

Henry, T. J., Backman, D. E., Blackwell, J., Okimura, T., & Jue, S. 2003, The Future of Small Telescopes in the New Millennium 3, Science in the Shadow of Giants, 289, 111, http://adsabs.harvard.edu/abs/2003ASSL..289..111H

Henry, T. J., Jao, W.-C., Subasavage, J. P., Beaulieu, T. D., Ianna, P. A., Costa, E., & Méndez, R. A. 2006, AJ, 132, 2360

Henry, T. J., Subasavage, J. P., Brown, M. A., Beaulieu, T. D., Jao, W., & Hambly, N. C. 2004, AJ, 128, 2460

Holberg, J. B., & Bergeron, P. 2006, AJ, 132, 1223

Holberg, J. B., Oswalt, T. D., & Sion, E. M. 2002, ApJ, 571, 512

Holberg, J. B., Sion, E. M., Oswalt, T., McCook, G. P., Foran, S., & Subasavage, J. P. 2008, AJ, 135, 1225

Iben, I., & Renzini, A. 1984, Phys. Rep., 105, 329

Jao, W.-C., Henry, T. J., Subasavage, J. P., Brown, M. A., Ianna, P. A., Bartlett, J. L., Costa, E., & Méndez, R. A. 2005, AJ, 129, 1954

Kawka, A., Vennes, S., Schmidt, G. D., Wickramasinghe, D. T., & Koch, R. 2007, ApJ, 654, 499

Kawka, A., Vennes, S., & Thorstensen, J. R. 2004, AJ, 127, 1702

Koerner, D. W., Henry, T. J., Fuhrman, L. A., Parker, C. C., Kaplan, I. J., Wei-Chun, J., & Subasavage, J. 2003, BAAS, 35, 1272

Landolt, A. U. 1992, AJ, 104, 340

Landolt, A. U. 2007, AJ, 133, 2502

Liebert, J., Bergeron, P., & Holberg, J. B. 2005, ApJS, 156, 47

Luyten, W. J. 1979a, LHS Catalogue (2nd ed.; Minneapolis, MN: Univ. of Minnesota Press)

Luyten, W. J. 1979b, New Luyten Catalogue of Stars with Proper Motions Larger than Two Tenths of an Arcsecond (Minneapolis, MN: Univ. Minnesota Press)

McCook, G. P., & Sion, E. M. 1999, ApJS, 121, 1

Oppenheimer, B. R., Hambly, N. C., Digby, A. P., Hodgkin, S. T., & Saumon, D. 2001, Science, 292, 698

Pauli, E.-M., Napiwotzki, R., Heber, U., Altmann, M., & Odenkirchen, M. 2006, A&A, 447, 173

Perryman, M. A. C., et al. 1997, A&A, 323, L49

Press, W. H., Teukolsky, S. A., Vetterling, W. T., & Flannery, B. P. 1992, Numerical Recipes in FORTRAN (2nd ed.; Cambridge: Cambridge Univ. Press), 644

Provencal, J. L., Shipman, H. L., Koester, D., Wesemael, F., & Bergeron, P. 2002, ApJ, 568, 324

Smart, R. L., et al. 2003, A&A, 404, 317

Subasavage, J. P., Henry, T. J., Bergeron, P., Dufour, P., Hambly, N. C., & Beaulieu, T. D. 2007, AJ, 134, 252 (Paper XIX)

Subasavage, J. P., Henry, T. J., Hambly, N. C., Brown, M. A., & Jao, W. 2005a, AJ, 129, 413

Subasavage, J. P., Henry, T. J., Hambly, N. C., Brown, M. A., Jao, W.-C., & Finch, C. T. 2005b, AJ, 130, 1658

van Altena, W. F., Lee, J. T., & Hoffleit, E. D. 1995, The General Catalogue of Trigonometric (Stellar) Parallaxes (4th ed., New Haven, CT: Yale Univ. Obs.) (completely revised and enlarged) http://adsabs.harvard.edu/abs/1995gcts.book.....V

van Leeuwen, F. 2007, *Hipparcos*, the New Reduction of the Raw Data (Astrophysics and Space Science Library) 350 (Dordrecht: Springer) http://adsabs.harvard.edu/abs/2007hnrr.book.....V

Vennes, S., & Kawka, A. 2003, ApJ, 586, L95

Wesemael, F., Greenstein, J. L., Liebert, J., Lamontagne, R., Fontaine, G., Bergeron, P., & Glaspey, J. W. 1993, PASP, 105, 761